RSC Advances

PAPER

View Article Online
View Journal | View Issue

Cite this: *RSC Adv.*, 2026, **16**, 14845

Structural and bactericidal properties of imidazolium ionic liquid-based micelles of thyme essential oil

Salma Mokni,[a] Walid M. Hassen,[a] Mayank,[a] Narinder Singh [b] and Jan J. Dubowski *[a]

Received 5th January 2026
Accepted 28th February 2026

DOI: 10.1039/d6ra00117c

rsc.li/rsc-advances

We report the structural and bactericidal properties of the imidazolium ionic liquid (IL)-based micelles of *Thymus capitatus* (thyme) essential oil (EO). The formation of micelles was investigated by contact angle measurements, which revealed a critical micelle concentration (CMC) of 2.5–3 μM for the IL mixed with thyme at 0.2 μL mL^{-1}. The size, stability and self-assembly of EO-IL micelles in water were evaluated by the dynamic light scattering technique. It was determined that the self-dispersed micelles with a ~400 nm diameter remained stable in a water environment for at least 6 months from their formation. The bactericidal properties of micelles investigated against *S. aureus* and *E. coli* under liquid-to-liquid conditions revealed a 6-log reduction in the bacterial concentration from 10^8 CFU mL^{-1} following 1 min exposure. Minimal bactericidal growth of both bacteria was observed under the CMC conditions. These results demonstrate the potential of EO-IL micelles as natural agents that self-disperse in water and kill bacteria at rapid rates.

1 Introduction

Essential oils (EOs) are highly concentrated volatile compounds extracted from various parts of plants, including leaves, flowers, stems, roots and fruits.[1] They are composed of a complex mixture of aromatic compounds, including terpenes, phenols and alcohols, and their chemical composition can vary considerably depending on the plant species, growing conditions and harvesting methods. EOs are widely used in aromatherapy and in the food,[1–3] cosmetics[4] and pharmaceutical[5–8] industries due to their unique flavours, fragrance and therapeutic properties. Recently, with the increased interest in the use of natural products, these compounds have attracted growing research attention owing to their antibacterial,[9–11] antifungal,[12] antiviral,[13] and insecticidal properties.[14] In addition to being proposed as corrosion inhibitors,[15] EOs can cause irreversible damage to bacterial cell walls and proteins and increase membrane permeability, causing leakage of its contents.[13] EOs can also affect bacterial functions by disrupting the functionality of their genetic material. The efficiency of bactericidal response to EOs depends on the oil composition, concentration and targeted microorganisms. Numerous studies have reported the antibacterial activity of different EOs against a wide range of Gram-positive and Gram-negative pathogenic bacteria.[16–21] The minimum bactericidal concentration (MBC) of one of the most frequently investigated EOs, thyme EO, ranges between 2.61 and 15.07 mg mL^{-1}.[22] This compound has been applied against foodborne pathogens, such as *S. aureus* (ATCC 25923), *L. monocytogenes* (ATCC 7644), *E. coli* (ATCC 25922), and *S. Typhimurium* (ATCC 14028).[22] However, despite the well-known bactericidal activities of many EOs, the major limitation related to their use as disinfectants is their hydrophobic nature, which makes them poorly dispersible in aqueous environments.[1,23] The lipophilic nature of EOs is due to the presence of terpenes, phenols, ketones and other compounds with nonpolar hydrocarbon chains that lead to poor dissolution in polar solvents like water. The encapsulation of EOs in micelles using surfactants is an attractive approach to ensure their dispersion in water. A surfactant is an amphiphilic molecule with a hydrophilic head and a hydrophobic chain, enabling it to reduce the surface tension and emulsify hydrophobic oils in water.[24] Micelles are formed at or above a specific surfactant concentration, called the critical micelle concentration (CMC).[25] While forming the micelles in water, the surfactant organizes itself with the hydrophilic head exposed to the aqueous environment and the hydrophobic tail directed inward. The resulting micelles are stabilized by van der Waals forces, hydrogen bonding and electrostatic interactions.[26] Table 1 presents examples of EO micelles formed in water with amphiphilic and non-ionic surfactants.

The non-ionic character of surfactants is not ideal for enhanced interaction with naturally negatively charged

[a]*Interdisciplinary Institute for Technological Innovation (3IT), Quantum Semiconductors and Photon-based BioNanotechnology Group, Laboratoire Nanotechnologies Nanosystèmes (LN2)-IRL3463, CNRS, Department of Electrical and Computer Engineering, Université de Sherbrooke, 3000, boul. de l'Université, Sherbrooke, Québec J1K 0A5, Canada. E-mail: jan.j.dubowski@usherbrooke.ca*

[b]*Department of Chemistry, Indian Institute of Technology Ropar, Punjab 140001, India*

Table 1 Examples of popular EO-surfactant micelles in water

EO	Surfactant	Polarity	Micelle diameter (nm)	CMC	Characterization technique	Ref.
Eucalyptus	Surfactin	Non-ionic	175 ± 18	40 mg L^{-1}	Surface tension dynamic	27
	PX407	Amphiphilic	30.6 ± 0.54	4 mM	light scattering	28
Oregano	Tween 80	Non-ionic	108–337	0.01 mM (38 ± 4) × 10^{-4}	Surface tension	29
	Tween 80	Non-ionic	24–68	% (w/w)	Surface tension	30
Anise	Tween 80	Non-ionic	153.7 ± 0.6	0.015 mM	Dynamic light scattering	31
Rosemary	Tween 20	Non-ionic	61.47	0.06 mM	Fluorescence intensity	32

bacteria. On the other hand, ionic liquids (ILs), used mainly in drug synthesis and drug delivery systems in the pharmaceutical and medical fields,[33] comprise an organic cationic head and an inorganic anionic tail. Due to their cationic head, they are of interest for the formation of bactericidal micelles and are attractive for their interaction with negatively charged bacterial cell walls. ILs, recently emerging as highly attractive materials for different applications,[34,35] have shown interesting physico-chemical and functional properties including low vapor pressure and high thermal and chemical stability. More importantly, the structural tunability of these surfactants allows precise modulation of some key properties such as their polarity, hydrophobicity and self-assembling behaviour.[36] Miscibility is another property of IL surfactants influencing their behaviour in aqueous solutions. For example, long-chain 1-alkyl-3-methylimidazolium compounds with $[CnMIM]^+$ groups have been proposed as surfactants due to their high capacity to form micelles in the presence of water.[37,38] The high affinity of ILs for oils has been explored in the oilfield industry as they can significantly reduce the tension at the oil–water interface, resulting in enhanced oil recovery.[39] Also, IL surfactants with high-carbon-number aliphatic chains allow the formation of stable micelles with low CMCs.[40] The bactericidal and virucidal properties of ILs have also been reported.[24,33,41] In fact, many cationic ILs exhibit antimicrobial activity mainly arising from their interaction with the bacterial membrane. This electrostatic interaction allows their integration into the lipid bilayer, inducing the disruption of the membrane integrity and enhancing its permeability, thus ultimately causing cell lysis. In this context, it has been shown that increasing the alkyl chain length enhances the antimicrobial potency of ILs, further illustrating the importance of molecular design and the advantages of the tuneable properties[42] of ILs. Such properties make ILs attractive to form bactericidal EO-IL micelles in water.

In this paper, we investigate the structural and bactericidal properties of EO-based micelles in water supported by cationic imidazolium IL surfactants. A schematic of the formation of EO-IL micelles designed for killing bacteria in water is illustrated in Scheme 1.

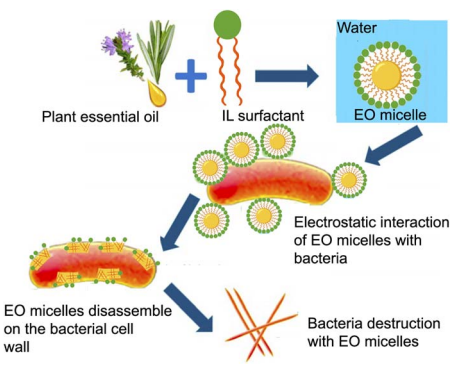

Scheme 1 Schematic of the formation of polarized EO-IL micelles designed for strong interactions and killing bacteria.

2 Experimental

2.1 Materials and reagents

Thymus capitatus (thyme) EO was extracted from natural Tunisian plants populations. Oil extraction was carried out from dried leaves that underwent water distillation for 3 hours using a Clevenger-type apparatus. The excess water was removed from thyme oil by drying over anhydrous sodium sulphate. No organic solvents were used for the extraction.[43,44] *Escherichia coli* (*E. coli*) K12 BW25113 (GFP *E. coli*) continually expressing the green fluorescent protein (GFP) and *Staphylococcus aureus* (*S. aureus*) ATCC 29213 were provided by, respectively, Prof. Sébastien Rodrigue and Prof. François Malouin, both from the Département de Biologie of the Université de Sherbrooke. The Luria-Bertani (LB) broth and agar were purchased from Sigma Aldrich. The IL formulation, 1,3-bis(2-(heptylamino)-2-oxoethyl)-1*H*-benzo[*d*]imidazole-3-ium bromide (IL-5), used in this study was provided by Prof. Narinder Singh (Department of Chemistry of the Indian Institute of Technology Ropar, Punjab, India). The molecular structure of IL-5 is presented in Scheme 2.

All solutions were prepared in deionised (DI) water and filtered through a 0.22 μm syringe filter.

2.2 Experimental details

2.2.1 Micelle synthesis. IL-EO micelles were prepared by first combining the required volumes of thyme EO and the IL in a clean container. The mixture was then diluted with filtered DI water to achieve the desired final concentrations of both components. The resulting mixture was homogenized by 10 seconds vortexing and, unless otherwise specified, used for dedicated experiments.

2.2.2 Micelle analysis. The CMC was determined by the contact angle (CA) technique using a Drop Shape Analyser (DSA25S KRUSS), viscosity measurements (NDJ-9S digital rotary viscometer, Aermanda, China) and UV spectrophotometry analysis with a Genesys 180 UV-visible spectrophotometer

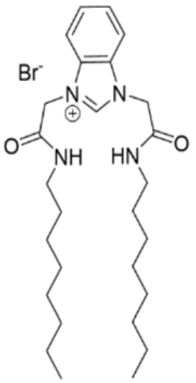

Scheme 2 Molecular structure of IL-5.

(Thermo Fisher, USA). A series of solutions with 0.2 μL of thyme EO in 1 mL of IL solutions with a concentration varying between 0.5 and 15 μM was prepared for each of the investigated methods.

For CA measurements, a ~1 μL drop was deposited on a 2 cm × 2 cm Teflon plate. The viscosity measurements were performed with a rotor immersed in 15 mL of solutions prepared in a falcon tube.

The optical density (OD) of EO-IL solutions was measured after determining the maximum absorbance wavelength (λ_{max}) from the wave scan between 200 and 800 nm for the preparation with 0.2 μL mL^{-1} thyme EO and 15 μM IL.

To determine the CMC, optical absorbance was measured at a fixed wavelength (λ_{max}) for different thyme EO-IL solutions prepared either by varying the concentration of the IL between 1.5 and 15 μM with the thyme EO concentration fixed at 0.2 μL mL^{-1} or by varying the concentration of thyme EO between 0.2 and 2 μL mL^{-1} with the IL concentration fixed at 2.5 μM.

The micelle size was determined using the NanoBrook 90Plus Particle Size Analyzer (Brookhaven Instruments Corporation, NH, USA) for freshly prepared IL solutions with concentrations varying between 1 and 15 μM and the thyme EO concentration fixed at 0.2 μL mL^{-1}. The concentration-dependent micelle size was investigated for the 1× CMC formulation (2.5 μM IL + 0.2 μL mL^{-1} thyme oil).

To evaluate the self-dispersion of EO-IL micelles, four formulations were prepared in duplicate in 15 mL falcon tubes at concentrations corresponding to 1×, 10×, 25× and 50× the CMC for the average value of the CMC determined with the three methods. All samples were prepared by diluting the IL solution at 500 μM with 0.2 μL mL^{-1} thyme EO. For each concentration, one tube was vortexed immediately after preparation, and the second tube was allowed to settle for 1 h without vortexing. The micelle size was measured *via* the DLS technique for both vortexed and non-vortexed solutions. The stability of micelles was investigated for up to 195 days.

2.2.3 Bactericidal activity study. Fresh cultures of *E. coli* and *S. aureus* from thawed aliquots were prepared in the LB agar before each experiment to evaluate the bactericidal activities of the thyme, IL, and thyme-IL mixture. After the growth, a few colonies were placed in water, and the concentration of bacteria was determined by OD measurements at 600 nm (OD_{600}). OD_{600} = 0.1 corresponds to 1 × 10^8 and 3 × 10^7 CFU mL^{-1} of *E. coli* and *S. aureus* bacteria, respectively.

To determine the MBC of thyme EO, multiple falcon tubes were prepared with *E. coli* and *S. aureus* suspensions at 10^8 CFU mL^{-1}. Then, thyme EO was added to each tube at concentrations ranging between 0.1 and 10 μL mL^{-1}. To determine the MBC of the IL, the suspension of either *S. aureus* or *E. coli* at 10^8 CFU mL^{-1} was added to different concentrations of the IL in DI water. In both experiments, the prepared tubes were vortexed for 30 seconds and allowed to settle for 1 minute. The bactericidal activity was evaluated by the viable bacterial cell culture method, which involved inoculating three LB agar Petri dishes with 100 μL of each tested suspension. After 24 hours of growth in the incubator at 35 °C, the number of colonies was counted to determine the rate of reduction of bacteria. The MBC for each case corresponds to the lowest concentration of the investigated solution allowing a 6-log reduction in the bacterial concentration.

To evaluate the MBC of EO-IL formulations, both components were mixed at concentrations lower than their individual MBCs. Subsequently, *S. aureus* or *E. coli* at 10^8 CFU mL^{-1} were added to different thyme EO-IL formulations and mixed by vortexing for 30 s, followed by 1 min incubation and consecutive culturing in the LB agar medium. The MBC of each thyme EO-IL formulation corresponds to the lowest concentration allowing a 6-log reduction compared with the reference experiment. The procedure applied for the evaluation of the bactericidal properties of EO-IL formulations is illustrated in Scheme 3.

3 Results and discussion

3.1 Determination of the critical micelle concentration

Fig. 1 presents the CA as a function of the IL concentration at a fixed thyme EO concentration of 0.2 μL per 1 mL of the solution. Two linear phases of decreasing CAs can be distinguished in this figure. The rapid decrease (phase one) in the CA

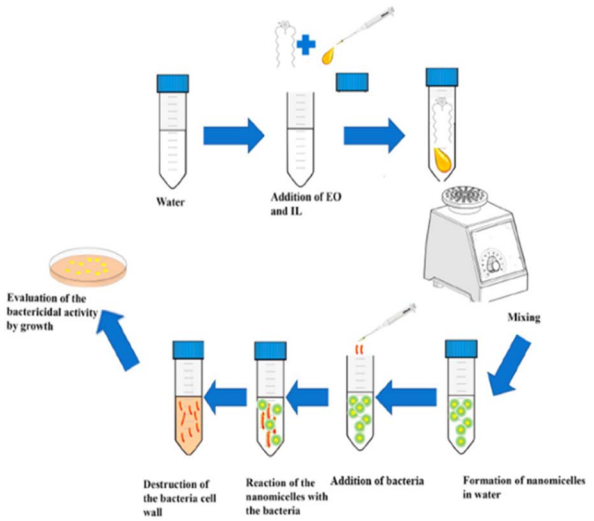

Scheme 3 Schematic of the procedure for determining the MBC of thyme EO-IL formulations.

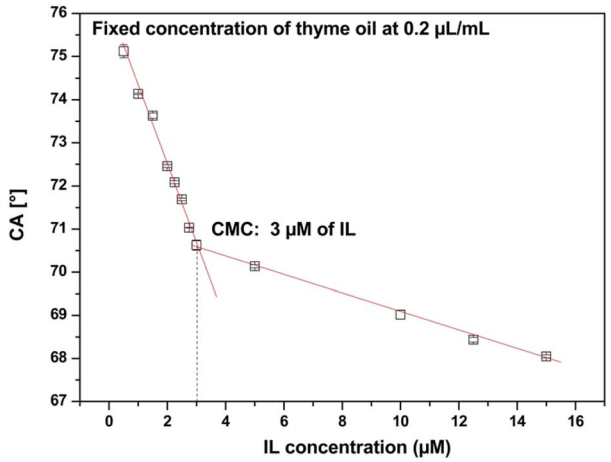

Fig. 1 Contact angle of EO-IL solutions *vs.* the concentration of the IL at a fixed concentration of thyme EO. The inflection point observed for the IL at 3 ± 0.07 µM relates to the CMC.

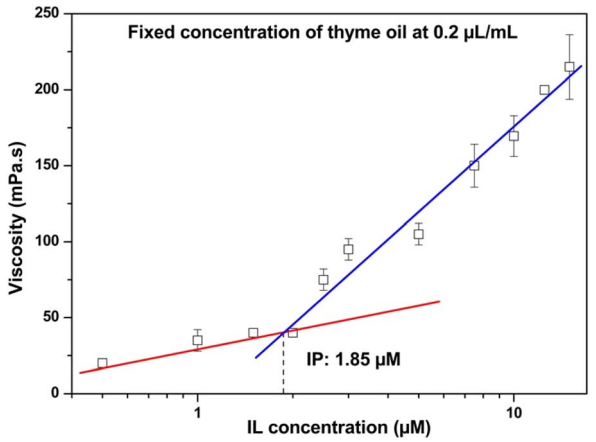

Fig. 2 Viscosity of thyme EO-IL at a fixed concentration of EO *vs.* the concentration of the IL.

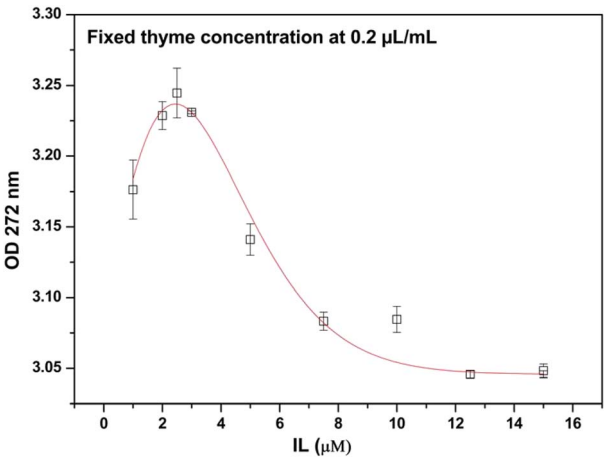

Fig. 3 Optical density at 272 nm measured for solutions with different concentrations of the IL and a fixed concentration of thyme EO.

with increasing concentration of the IL is consistent with a systematic reduction in the liquid surface tension.[45] In the second phase, for IL concentrations ≥ 3 µM, the slower decrease in CA values is consistent with micelle formation and, consequently, with a reduced rate of decrease in the liquid surface tension.[46] The intersection of the plots representing both phases is indicated by the inflection point, which relates to the CMC. Sedaghat Doost *et al.*[47] applied this method to determine the CMC at 10 µM of the Tween 80 surfactant mixed with high-oleic sunflower oil. This CMC was only slightly lower than that of Tween 80 alone (~12–15 µM). Our results illustrate formation of EO-IL micelles at the IL-5 (surfactant) concentration of ~3 µM, which compares to CMC of IL-5 alone at 148 µM.

The viscosity of EO-IL formulations as a function of the IL concentration for solutions formulated with a fixed thyme EO concentration of 0.2 µL per 1 mL of the solution is plotted in Fig. 2. The intersection of the two differently inclined lines of the semi-logarithmic plots observed in this figure defines the CMC value.[48] Our experiment reveals that the CMC of the IL is 2.32 ± 0.941 µM (n = 3), which is in a reasonable agreement with the CMC obtained by the CA measurements. The viscosity measurements have been previously employed for the research on the formation of IL-based micelles.[38] Shah *et al.* used this technique to determine that the CMCs of dodecyltrimethylammonium bromide (DTAB) and cetyltrimethylammonium bromide surfactants are 14.3 mM and 1.2 mM, respectively,[48] which are significantly greater than the surfactant concentrations observed in our experiments.

The results of the OD measurements at 272 nm as a function of the IL concentration at a fixed thyme EO concentration of 0.2 µL mL^{-1} are shown in Fig. 3. Qualitatively, similar dependence is also observed for the OD measurements carried out at 230 nm. The OD maximum (OD_{max}) observed in Fig. 3 for the IL at 2.75 µM is compared with that of the IL at 3.1 µM determined under 230 nm irradiation (SI, Fig. S1). The formation of the OD_{max} is related to the initial increase in the concentration of the light-scattering centres that comprise IL monomers attached to the EO microdroplets. Upon the onset of the formation of micelles, *i.e.*, at the CMC point, the optical scattering begins to decrease because more uniform and stable micelles begin to form. The addition of IL molecules does not significantly affect the absorbance thanks to the hydrophilicity of the Br^- counterion of the investigated IL, which also promotes the stability of micelles.[49] At this stage, the injection of the IL further dilutes the solution, contributing to the increased transparency of the investigated suspension. We note that the IL concentration defined by the OD_{max} correlates well with the CMCs determined by CA and viscosity measurements.

The results of the OD measurements at a fixed IL concentration of 2.5 µM and varying concentrations of thyme EO are shown in Fig. 4. The saturation character of this dependence is illustrated with the fitting curve (dotted line), while the intersection of the two tangential lines defines the inflection point associated with the CMC. The CMC of 0.42 µL mL^{-1} determined from this experiment compares with the CMC of 0.51 µL mL^{-1} obtained from the optical absorption experiment carried out

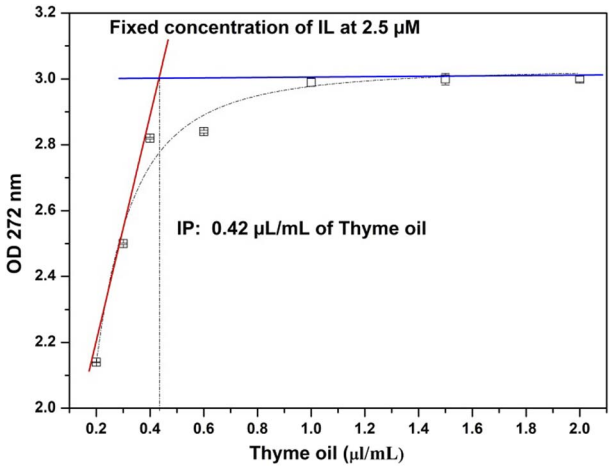

Fig. 4 Optical density at 272 nm for a fixed concentration of the IL *vs.* the concentration of thyme EO.

under 230 nm irradiation (SI, Fig. S2). The saturation of the OD with increasing concentration of EO seems be related to the increasing concentration of oil microdroplets. Upon reaching the CMC, stable micelles are formed, and the extra EO is incorporated into their hydrophobic core, causing them to expand and swell. The saturation of the OD is consistent with the formation of a thermodynamically stable microemulsion.[50]

3.2 Micelle size characterization

The results of the micelle size measurements by DLS in solutions with IL concentrations ranging between 1 and 15 μM and a fixed thyme EO concentration of 0.2 μL mL^{-1} are summarized in Table 2. We observe that for all the tested solutions, the size of micelles ranges between 320 and 414 nm. The lowest standard deviation of 8.5 nm is observed for the solution with an IL concentration of 2.5 μM and a thyme EO concentration of 0.2 μL mL^{-1}. These results suggest that the formation of the most uniform and, potentially, most stable micelles takes place at the CMC determined *via* CA, viscosity and spectrophotometry experiments (Fig. 1–3).

Furthermore, the weak dependence of the DLS hydrodynamic diameter of micelles on the IL concentration, as observed in Table 3, indicates that an increased IL concentration leads to the formation of a higher number density of EO-swollen micelles rather than the significant growth of individual aggregates.[51]

Table 2 IL-dependent average sizes of micelles for thyme EO at 0.2 μL mL^{-1}

	IL concentration μM	Micelle size nm	SD nm
0.2 μL mL^{-1} of thyme EO	1	375	30.1
	1.5	353	12
	2	320	13.4
	2.5	381	8.5
	3	348	36.4
	5	375	32.5
	10	414	37.4
	12.5	363	31.8
	15	366	11.3

Table 3 Average micelle size obtained from the dilution of concentrated preparations. 1× corresponds to 2.5 μM IL + 0.2 μL mL^{-1} thyme EO

Initial concentration	Final concentration after dilution	Micelle size (nm)
Vortexed		
10×	1× dilution	367 ± 33.7
25×	1× dilution	270 ± 14.7
50×	1× dilution	293 ± 14.4
Non-vortexed (1 h of dispersion)		
10×	1× dilution	418 ± 24.3
25×	1× dilution	326 ± 37.8
50×	1× dilution	510 ± 52.3

3.3 Stability and self-assembly of thyme EO-IL micelles

The DLS-determined average sizes of the micelles at 1× CMC prepared from formulations concentrated at 10×, 25×, and 50× CMC are presented in Table 3. The vortexed solutions produced micelles with the average size ranging between 270 and 370 nm. In comparison, the non-vortexed samples, following 1 h of self-dispersion in water, yielded micelles with the average size between 326 and 510 nm. It appears that less-dispersed micelles with an average ~300 nm diameter are produced by vortexing after diluting from the concentrated oil-IL solutions.

A comparison between vortexed and non-vortexed samples prepared directly by mixing the IL and thyme EO at concentrations corresponding to 1×, 10×, 25× and 50× the CMC is presented in Fig. 5. Initially, up to 14 days, the vortexed preparations showed micelles with largely dispersed dimensions ranging between 250 and 2800 nm (Fig. 5a), while the non-vortexed samples revealed micelles with dimensions between 200 and 400 nm, (Fig. 5b). The average dimension of these micelles, except for the 50× micelles, weakly depended on the aging process. This was also true for the vortexed samples aged for more than 25 days. The average size of the micelles in the 50× vortexed solutions after 25 days dropped from 2800 to 1250 nm and increased again to 1500 nm after 190 days. A significantly weaker variation in the micelles' dimensions was observed for the 50× non-vortexed solution. These results suggest that vortexing of concentrated samples is not advantageous to produce assemblies of relatively uniform thyme EO-IL micelles. Furthermore, working with the largely concentrated solutions (50×) results in less uniform micelles, and vortexing does not seem to reduce the dispersion in the size of these micelles. This observation is consistent with the literature data reporting that self-assembled micelles display a smaller size, easier preparation, and efficient solubilisation.[52] Indeed, a strong applied mechanical force might induce non-uniformed micelle dispersion and collapsing of some of the micelles assembled in large aggregates. In the absence of vortexing, the

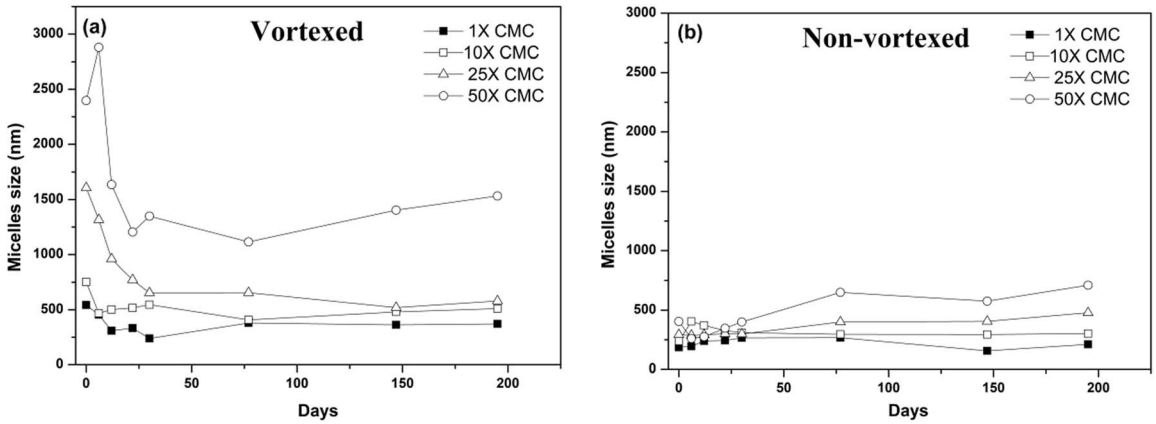

Fig. 5 Micelle size variation over a 95 days period for vortexed (a) and non-vortexed (b) thyme EO-IL preparations.

positively charged IL-thyme micelles self-disperse in water due to the repulsive forces and form naturally more uniform formulations.

3.4 Bactericidal properties of thyme EO-IL micelles

The MBC values of *E. coli* and *S. aureus* at 10^8 CFU mL^{-1} exposed to thyme oil, the IL, and a combination of thyme oil-IL solutions are presented in Table 4. We can see that an equal concentration of the thyme solution of 0.5 μL mL^{-1} is required to achieve a 6-log reduction in *E. coli* or *S. aureus* suspensions at 10^8 CFU mL^{-1} following 1 min exposure. *Thymus capitatus*, the thyme species used in this research, like other thyme plants, is found to have highly antibacterial properties against four Gram-negative bacteria, including *S. Typhimurium*, and four Gram-positive bacteria, including *L. monocytogenes*.[53] Thyme EO is particularly rich in thymol and carvacrol,[54] which exhibit high antibactericidal activity due to their ability to block the NorA Efflux Pump.[55,56] This results in the inability of bacteria to efflux toxic chemicals from the cell.[57] Under IL-only conditions, IL concentrations of 5 and 100 μM were required to achieve a similar result against *S. aureus*, a Gram-positive bacteria, and *E. coli*, a Gram-negative bacteria, respectively.

Gram-positive bacteria with a thick peptidoglycan layer can be easily disrupted by the IL, while Gram-negative bacteria have an outer membrane that provides an additional barrier against surfactant penetration.[58] The bactericidal activity of the IL begins by the electrostatic adsorption of its cationic head by the bacterial membrane. This leads to the disorganization of the phospholipid double layer and leaking out of the intracellular cytoplasm, which destructs the cell wall by the lysing process.[59] Generally, the MBCs of different ILs are found much higher than the MBC of the IL reported in this publication. For example, the 1-decyl-3-methylimidazolium bromide IL with a single 10-carbon aliphatic chain shows an MBC of 1 mM against *S. aureus*,[42] which is much higher than the 5 μM MBC observed in our experiments. Panda *et al.*[60] also studied the bactericidal activity of ILs with different alkyl chain lengths against *E. coli* and *S. aureus* strains. Their results showed MBC values ranging from 5 μM to 50 μM for *S. aureus* and 10 μM to 50 μM for *E. coli*. This difference in the IL bactericidal efficiency might be related to the "side-chain effect" of the cation and the respective chaotropicity of IL anions. Generally, longer and more hydrophobic side chains tend to increase the toxicity of the IL[61] and promote the formation of stable micelles at low CMCs.[40] A comparable bactericidal activity of the IL and conventional surfactants, such as CTAB, was also reported in the literature. For instance, Li *et al.*[62] reported the MBCs of a series of polymerizable quaternary ammonium surfactants (QASs), including CTAB, against *Staphylococcus aureus* and *Escherichia coli* and demonstrated their bactericidal activity in a comparable range with our IL against these bacteria, with *E. coli* clearly requiring higher concentrations of the IL. The comparable MBC values are likely due to the resemblance of the surfactant structures and the presence of a cationic head, which facilitates the interaction with bacteria.

Regarding the bactericidal properties of the individual IL and EO components, the concentration of thyme EO applied together with the IL was reduced by 2.5×, and that of the IL by 40×. This illustrates the strong synergism of the investigated products. The possible mechanism behind this synergism is related to the electrostatically supported delivery of a high concentration of antibacterial agents, forming direct contact with bacteria. Zhang *et al.*,[63] who investigated clove/cinnamon EO emulsions as natural antimicrobial agents in the food industry, have also reported a strong synergism for formulations based on benzalkonium chloride (BAC) or didecyldimethylammonium chloride (DDAC) against *E. coli*. When used alone, the MBCs of eugenol and BAC are 3.2 at mg mL^{-1} and 0.064 mg mL^{-1}, respectively. When combined, an MBC of 0.8 mg mL^{-1} for eugenol + 0.016 mg mL^{-1} for BAC was observed, corresponding to a 4× reduction in the

Table 4 MBCs of thyme EO, the IL and thyme EO-IL for the 6-log reduction in the bacterial concentration

	S. aureus	*E. coli*
Thyme oil (μL mL^{-1})	0.5	0.5
IL (μM)	5	100
Thyme oil (μL mL^{-1}) + IL (μM)	0.2 + 2.5	0.2 + 2.5

concentrations of the two investigated compounds. The DDAC alone reveals the MBC at 0.004 mg mL^{-1}, but when mixed with eugenol, its concentration is reduced by 8×.[64] Xu *et al.*[65] also reported that nanoemulsion formulations based on cinnamon essential oil and the cationic lauric arginate surfactant considerably enhance the antimicrobial activity and show a synergistic antibacterial effect against *S. aureus*.[65]

4 Conclusion

We have investigated conditions for the formation of swollen micelles comprising thyme EO and the 1,3-bis(2-(heptylamino)-2-oxoethyl)-1*H*-benzo[*d*]imidazole-3-ium bromide IL. The choice of the IL was dictated by its cationic character and potential for biodegradation. The inflection points observed in CA (Fig. 1) and viscosity (Fig. 2) measurements as a function of the IL concentration, together with the saturation of the EO solubilization capacity (Fig. 4), indicate the onset of IL-mediated micellar growth and EO-swollen micelle formation. This growth is further confirmed by a weak dependence of the DLS hydrodynamic diameter on the IL concentration (Table 3), which indicates that an increased concentration of the IL leads to the formation of a higher number density of EO-swollen micelles rather than significant growth of individual aggregates. In addition, the DLS analysis reveals that swollen micelles with an average diameter of 250 nm are stable up to at least 190 days if produced from solutions concentrated up to 25× beyond their CMC values.

The MBC, determined at 2.5 μM IL + 0.2 μL mL^{-1} thyme for a 6-log reduction of *E. coli* or *S. aureus* suspensions following 1 min exposure, correlates well with the CMC value. Compared with the bactericidal properties of the investigated thyme EO and IL, our results demonstrated the synergistic effect manifested by the reduced concentration of both components applied simultaneously for rapidly killing bacteria. This synergism is attributed to the enhanced efficiency in delivering EO to the surface of bacteria and supported by the electrostatic attraction of the IL-polarized swollen micelles. The process is further enhanced by the bactericidal properties of the IL alone. The application of cationic IL surfactants to form swollen bactericidal micelles self-dispersing in water is a promising approach towards the development of biodegradable disinfectants against the proliferation of bacteria.

Author contributions

Salma Mokni: performing the experiments, analysing the data, and writing the manuscript. Walid M. Hassan: supervising the project, contributing to the experiments, assisting with data analysis, and reviewing and editing the manuscript. Mayank: designing ILs and reviewing the manuscript. Narinder Singh: designing and providing ILs and reviewing the manuscript. Jan J. Dubowski: supervising the project, assisting with data interpretation, providing critical feedback and reviewing and editing the manuscript. All authors read and approved the final manuscript.

Conflicts of interest

The authors declare that there are no conflicts of interest.

Data availability

All data supporting the findings of this study are included within the article and its supplementary information (SI). Supplementary information: optical density at 230 nm for EO-IL solutions *vs.* IL concentrations, and optical density at 230 nm for EO-IL solutions *vs.* thyme EO concentrations data. See DOI: https://doi.org/10.1039/d6ra00117c.

Acknowledgements

The funding for this research was provided by AXELYS Canada (Project AXE-0081), TransferTech (Sherbrooke), Sani-Marc Inc. (Victoriaville, Quebec), and the Natural Sciences and Engineering Research Council of Canada (NSERC, Discovery Grant RGPIN-2020-05558). The help provided by the technical staff of the Université de Sherbrooke Interdisciplinary Institute for Technological Innovation (3IT) is greatly appreciated.

References

1 M. I. S. Santos, C. Marques, J. Mota, L. Pedroso and A. Lima, *Microorganisms*, 2022, 10.
2 H. Benkhoud, Y. M'Rabet, M. Gara ali, M. Mezni and K. Hosni, *J. Food Process. Preserv.*, 2022, **46**, e15379.
3 T. Mićović, D. Topalović, L. Živković, B. Spremo-Potparević, V. Jakovljević, S. Matić, S. Popović, D. Baskić, D. Stešević, S. Samardžić, D. Stojanović and Z. Maksimović, *Plants*, 2021, **10**, 711.
4 B. Zuo, S. Li, Z. Guo, J. Zhang and C. Chen, *Anal. Chem.*, 2004, **76**, 3536–3540.
5 M. Jardak, J. Elloumi-Mseddi, S. Aifa and S. Mnif, *Lipids in Health and Disease*, 2017, **16**, 190.
6 Y. Abo-Zeid, M. R. Bakkar, G. E. Elkhouly, N. R. Raya and D. Zaafar, *Antibiotics*, 2022, 11.
7 K. Kunihiro, Y. Kikuchi, S. Nojima and T. Myoda, *Flavour Fragrance J.*, 2022, **37**, 210–218.
8 N. Rasool, Z. Saeed, M. Pervaiz, F. Ali, U. Younas, R. Bashir, S. M. Bukhari, R. R. Mahmood khan, S. Jelani and R. Sikandar, *Biocatal. Agric. Biotechnol.*, 2022, **44**, 102470.
9 D. H. Gilling, S. Ravishankar and K. R. Bright, *J. Environ. Sci. Health A Tox. Hazard. Subst. Environ. Eng.*, 2019, **54**, 608–616.
10 X. Zhang, J. Wang, H. Zhu, J. Wang and H. Zhang, *Chem. Biodivers.*, 2022, **19**, e202100951.
11 J.-H. Kang and K. B. Song, *Innov. Food Sci. Emerg. Technol.*, 2018, **45**, 447–454.
12 Y. S. Bae and M. S. Rhee, *Cell. Physiol. Biochem.*, 2019, **53**, 285–300.
13 T. J. Cho, S. M. Park, H. Yu, G. H. Seo, H. W. Kim, S. A. Kim and M. S. Rhee, *Molecules*, 2020, **25**, 1752.
14 I. Sadraoui-Ajmi, R. Sadraoui, G. Fatma, A. Soltani, R. Amari, S. Chaib, E. Boushih, A. Fajraoui and J. Mediouni Ben Jemâa, *Int. J. Environ. Res.*, 2023, **17**, 47.

15 C. Verma, D. S. Chauhan, R. Aslam, P. Banerjee, J. Aslam, T. W. Quadri, S. Zehra, D. K. Verma, M. A. Quraishi, S. Dubey, A. AlFantazi and T. Rasheed, *Green Chem.*, 2024, **26**, 4270–4357.
16 X. N. Yang, I. Khan and S. C. Kang, *Asian Pac. J. Trop. Med.*, 2015, **8**, 694–700.
17 Y. Zhang, X. Liu, Y. Wang, P. Jiang and S. Quek, *Food Control*, 2016, **59**, 282–289.
18 D. Huang, J. Xu, J. Liu, H. Zhang and Q. Hu, *Microbiology*, 2014, **83**, 357–365.
19 M. Nikolić, K. K. Jovanović, T. Marković, D. Marković, N. Gligorijević, S. Radulović and M. Soković, *Ind. Crops Prod.*, 2014, **61**, 225–232.
20 L. Degrand, R. Garcia, K. Crouvisier Urion and W. Guiga, *J. Mol. Liq.*, 2023, **388**, 122670.
21 A. Baicus, F. Mattuzzi, P. Ana-Maria, R.-S. Dinu, M. Dumitrescu, A.-A. Marinescu, D. Ionescu and D. Dragos, *Rev. Rom. Med. Lab.*, 2022, **30**, 327–338.
22 J. Milagres de Almeida, B. Crippa, V. Souza, V. Alonso, E. Júnior, C. Picone, A. Prata and N. Silva, *Food Control*, 2022, **144**, 109356.
23 I. D. Zlotnikov, A. A. Ezhov, M. A. Vigovskiy, O. A. Grigorieva, U. D. Dyachkova, N. G. Belogurova and E. V. Kudryashova, *Diagnostics*, 2023, **13**, 698.
24 S. De, S. Malik, A. Ghosh, R. Saha and B. Saha, *RSC Adv.*, 2015, **5**, 65757–65767.
25 D. R. Perinelli, M. Cespi, N. Lorusso, G. F. Palmieri, G. Bonacucina and P. Blasi, *Langmuir*, 2020, **36**, 5745–5753.
26 P. Shi, H. Zhang, L. Lin, C. Song, Q. Chen and Z. Li, *RSC Adv.*, 2019, **9**, 3224–3231.
27 R. Fopase, S. Pathode, S. Sharma, P. Datta and L. Pandey, *Polym.-Plast. Technol. Mater.*, 2020, **59**, 1–11.
28 H. Hashemi, M. Hashemi, S. Talcott, A. Castillo, T. Taylor and M. Akbulut, *ACS Food Sci. Technol.*, 2022, **2**, 290–301.
29 A. Sedaghat Doost, F. Devlieghere, C. V. Stevens, M. Claeys and P. Van der Meeren, *Food Chem.*, 2020, **327**, 126970.
30 A. Delmonte, F. F. Visentini, J. L. Fernández, L. G. Santiago and A. A. Perez, *Colloids Surf. B Biointerfaces*, 2024, **235**, 113783.
31 F. Alderees, S. Akter, R. Mereddy and Y. Sultanbawa, *J. Food Saf.*, 2022, **42**, e13001.
32 S. Park, S. Mun and Y. R. Kim, *Food Sci. Biotechnol.*, 2020, **29**, 1373–1380.
33 J. Wu, Q. Shu, Y. Niu, Y. Jiao and Q. Chen, *J. Agric. Food Chem.*, 2018, **66**, 7006–7014.
34 P. Verdía Barbará, H. Choudhary, P. S. Nakasu, A. Al-Ghatta, Y. Han, C. Hopson, R. I. Aravena, D. K. Mishra, A. Ovejero-Pérez, B. A. Simmons and J. P. Hallett, *Chem. Rev.*, 2025, **125**, 5461–5583.
35 J. Dupont, B. C. Leal, P. Lozano, A. L. Monteiro, P. Migowski and J. D. Scholten, *Chem. Rev.*, 2024, **124**, 5227–5420.
36 Z. Lei, C. Dai, J. Hallett and M. Shiflett, *Chem. Rev.*, 2024, **124**, 7533–7535.
37 N. Baccile, C. Seyrig, A. Poirier, S. Alonso-de Castro, S. L. K. W. Roelants and S. Abel, *Green Chem.*, 2021, **23**, 3842–3944.
38 J. M. Vicent-Luna, J. M. Romero-Enrique, S. Calero and J. A. Anta, *J. Phys. Chem. B*, 2017, **121**, 8348–8358.
39 J. Sun, Z. Xiu, L. Li, K. Lv, X. Zhang, Z. Wang, Z. Dai, Z. Xu, N. Huang and J. Liu, *Petroleum*, 2024, **10**, 11–18.
40 J. Łuczak, J. Hupka, J. Thöming and C. Jungnickel, *Colloids Surf., A*, 2008, **329**, 125–133.
41 N. Nikfarjam, M. Ghomi, T. Agarwal, M. Hassanpour, E. Sharifi, D. Khorsandi, M. Khan, F. Rossi, A. Rossetti, E. Zare, N. Rabiee, D. Afshar, M. Vosough, T. Maiti, V. Mattoli, E. Lichtfouse, F. Tay and P. Makvandi, *Adv. Funct. Mater.*, 2021, **31**, 57.
42 V. K. Sharma, J. Gupta, J. B. Mitra, H. Srinivasan, V. G. Sakai, S. K. Ghosh and S. Mitra, *J. Phys. Chem. Lett.*, 2024, **15**, 7075–7083.
43 E. Ameur, M. E. Sarra, k. Takoua, K. Mariem, A. Nabil, F. Lynen and K. M. Larbi, *Ind. Crops Prod.*, 2022, **180**, 114688.
44 M. Khouja, A. Elaissi, H. Ghazghazi, M. Boussaid, M. L. Khouja, A. Khaldi and C. Messaoud, *J. Essent. Oil Bear. Plants*, 2021, **23**, 1450–1462.
45 S. R. Shadizadeh and M. Amirpour, *Energy Sources, Part A Recovery, Util. Environ. Eff.*, 2017, **45**, 1–7.
46 M. Y. Alkawareek, B. M. Akkelah, S. M. Mansour, H. M. Amro, S. R. Abulateefeh and A. M. Alkilany, *J. Chem. Educ.*, 2018, **95**, 2227–2232.
47 A. Sedaghat Doost, C. V. Stevens, M. Claeys and P. Van Der Meeren, *Langmuir*, 2019, **35**, 10572–10581.
48 S. K. Shah, S. K. Chatterjee and A. Bhattarai, *J. Chem.*, 2016, **2016**, 2176769.
49 M. A. Rather, G. M. Rather, S. A. Pandit, S. A. Bhat and M. A. Bhat, *Talanta*, 2015, **131**, 55–58.
50 B. Wen, Z. Fu, D. Li, Z. Luo and B. Bai, *Phys. Fluids*, 2025, **37**, 102004.
51 A. Kadiri, T. Fergoug, K. O. Sebakhy, Y. Bouhadda, R. Aribi, F. Yssaad, Z. Daikh, M. El Hariri El Nokab and P. H. M. Van Steenberge, *ACS Omega*, 2023, **8**, 47714–47722.
52 M. Ghezzi, S. Pescina, C. Padula, P. Santi, E. Del Favero, L. Cantù and S. Nicoli, *J. Controlled Release*, 2021, **332**, 312–336.
53 E. Maniki, D. Kostoglou, N. Paterakis, A. Nikolaou, Y. Kourkoutas, A. Papachristoforou and E. Giaouris, *Molecules*, 2023, **28**, 1154.
54 M. B. Goudjil, S. Zighmi, D. Hamada, Z. Mahcene, S. E. Bencheikh and S. Ladjel, *J. S. Afr. Bot.*, 2020, **128**, 274–282.
55 J. Xu, F. Zhou, B. P. Ji, R. S. Pei and N. Xu, *Lett. Appl. Microbiol.*, 2008, **47**, 174–179.
56 K. Kachur and Z. Suntres, *Crit. Rev. Food Sci. Nutr.*, 2020, **60**, 3042–3053.
57 C. R. Dos Santos Barbosa, J. R. Scherf, T. S. de Freitas, I. R. A. de Menezes, R. L. S. Pereira, J. F. S. Dos Santos, S. S. P. de Jesus, T. P. Lopes, Z. de Sousa Silveira, C. D. de Morais Oliveira-Tintino, J. P. S. Júnior, H. D. M. Coutinho, S. R. Tintino and F. A. B. da Cunha, *J. Bioenerg. Biomembr.*, 2021, **53**, 489–498.
58 J. B. Gurtler, *J. Food Prot.*, 2020, **83**, 637–643.
59 N. Nikfarjam, M. Ghomi, T. Agarwal, M. Hassanpour, E. Sharifi, D. Khorsandi, M. Ali Khan, F. Rossi, A. Rossetti,

E. Nazarzadeh Zare, N. Rabiee, D. Afshar, M. Vosough, T. Kumar Maiti, V. Mattoli, E. Lichtfouse, F. R. Tay and P. Makvandi, *Adv. Funct. Mater.*, 2021, **31**, 2104148.

60 I. Panda, S. Raut, S. K. Samal, S. K. Behera and S. Pradhan, *Comput. Biol. Chem.*, 2025, **115**, 108288.

61 P. Mester, M. Wagner and P. Rossmanith, *Ecotoxicol. Environ. Saf.*, 2015, **111**, 96–101.

62 C. Li, J. Zhong, Y. Weng, S. Xie, S. Li and D. Yu, *RSC Appl. Interfaces*, 2025, **2**, 1690–1701.

63 S. Zhang, M. Zhang, Z. Fang and Y. Liu, *LWT–Food Sci. Technol.*, 2017, **75**, 316–322.

64 A. Pedreira, S. Fernandes, M. Simões, M. R. García and J. A. Vázquez, *Foods*, 2024, **13**, 1831.

65 Y. Xu, C. Gao, K. Hou, Y. Zhang, Y. Chen, X. Feng and X. Tang, *J. Future Foods*, 2026, **6**, 82–89.